

# A FREQUENCY-DOMAIN ANALYSIS OF VARISTOR CURRENT UNDER DISTORTED SUPPLY VOLTAGE

P. Bokoro\*, I. Jandrell\* and M. Hove\*\*

\* School of Electrical and Information Engineering, University of the Witwatersrand, Private Bag 3, Wits 2050, South Africa, E-mail: [688331@students.wits.ac.za](mailto:688331@students.wits.ac.za), E-mail: [ian.jandrell@wits.ac.za](mailto:ian.jandrell@wits.ac.za)

\*\* Dept. of Electrical and Electronic Engineering Science, University of Johannesburg, Private Bag 524, Auckland Park, South Africa, E-mail: [mhove@uj.ac.za](mailto:mhove@uj.ac.za)

**Abstract:** In this paper, the impact of supply voltage harmonics on the third harmonic current-based condition assessment of varistor is experimentally verified. Therefore, time-domain current and voltage waveforms, measured from ten identical varistor samples, are decomposed in frequency-domain. The flattop window of the FFT technique is used to determine the rms values and subsequently the third harmonic amplitude of the varistor current, before and after injection of harmonics. The harmonic-generating load consists of a triac-based ac voltage controller driving a resistive load unit at fixed firing angle of 10 degrees. All varistor devices used in this work were subjected to rated ac operating voltage. However, the results obtained indicated that the operation of a harmonic source connected across the varistor arrester has the effect of increasing the magnitude of the third harmonic component of the varistor current.

**Keywords:** Varistor arresters, third harmonic current, harmonics injection, time-domain waveform, frequency-domain waveform.

## 1. INTRODUCTION

The third harmonic component of the varistor current provides critical information relative to the condition of varistor devices [1, 2]. The key role of arresters in modern electrical or data circuits [3], justifies the recommended removal of degraded or aged arresters from service, in a bid to curb any chances of reduced protection or catastrophic failure of sensitive equipment. The third harmonic current (THC)-based assessment is often relied upon to monitor signs of degradation or ageing [4, 5]. Based on time-domain waveforms obtained mainly from Matlab simulation works, Jaroszewsky et al reported the negative influence of voltage harmonics on the leakage current measurement [6]. This finding is experimentally verified in this work with low voltage varistor units operating under harmonics distorted supply voltage. The time-domain current and voltage measured before and after harmonics injection, are decomposed in the frequency-domain using fast fourier transform (FFT) methodology. The frequency components obtained are analysed using the Flattop window technique of the FFT. For the purpose of this work, varistor samples and a triac-based ac voltage controller, are both connected in parallel to an ac voltage source. The voltage controller, which is driving a fixed resistive load across its output, is used as a harmonic source with third harmonic being the predominant component [7]. The supply voltage is set to operate at normal continuous rated voltage of varistor devices.

The flattop window analysis of the current spectra obtained before and after harmonics injection suggests that the injection of third harmonics on the system voltage causes the third harmonic component to be inflated without necessarily indicating the ageing of

arresters, and therefore renders the THC-based condition assessment of varistor arresters misleading.

## 2. METHODOLOGY

### 2.1 Description of the Test Regime

To meet the objectives of this work, a test regime enabling varistor arresters to be sequentially subjected to distorted and clean ac voltage was built. The test system consisted of a 0-250 V, 50 Hz variable ac voltage source supplying a triac-based ac voltage controller and a low voltage varistor unit. The voltage controller drives a fixed resistive load. For measurement and display purposes of scaled down time-domain current and voltage waveforms, the 2.5 VA stromwandler 4NA1104-OCB20 10/1 A current transformer (CT) with a 10W/1k $\Omega$  resistor connected across its output, is used to monitor the varistor current. The voltage across the varistor is measured through a 14 VA 220/24 V transformer. The waveforms thus obtained are captured using the TDS 1001B Tektronix digital scope. Channel 1 of the scope is used to display the current signal whereas channel 2 is dedicated to the voltage signal. The rms readings of the current flowing through and the voltage across the varistor are also obtained with the aid of the Fluke 289 and the Escort-EDM 82 digital meters respectively. The supply voltage is monitored using the YF-3120 digital meter. The test set up is depicted in figure 1.

### 2.2 Harmonic Source

The switching element of the ac voltage controller consists of 600 V, insulated TO-220 general purpose triac, which in fact is a combination of two thyristors mounted in antiparallel. To effect harmonic distortion in

the set up described above, the triac is preferentially fired at 10 degrees mark to enable distorted current to be drawn through, and thus distorting the voltage across the varistor. The voltage across the resistive load, which is directly proportional to the current through the load, is also measured through a 14 VA 220/24 V transformer. The waveforms of the voltage appearing across the varistor samples before and after harmonics injection are given in figure 2.

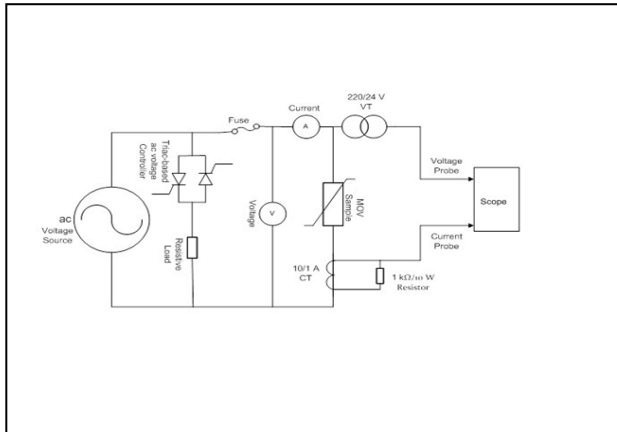


Figure 1: Experimental set up

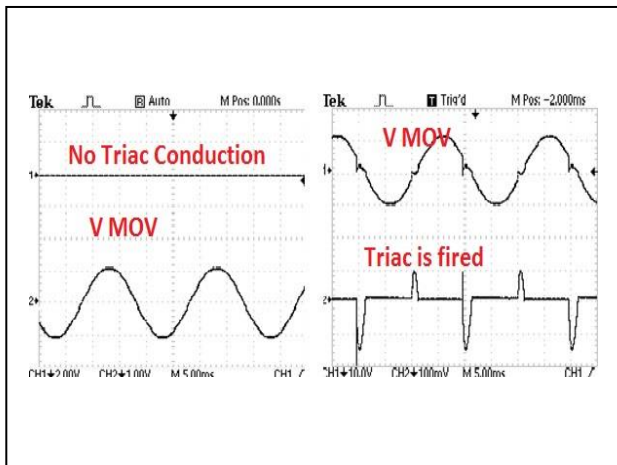


Figure 2: Varistor voltage before and after harmonics injection

### 3. FAST FOURIER TRANSFORM TECHNIQUE

Computer programs and digital instrumentation are continuously used in data acquisition or waveform recording and analysis. This justifies the need for discrete fourier transform (DFT) algorithms. The most preferred and utilised DFT approach is the FFT calculation which provides reduced amount of computation time involved. The FFT technique firstly decomposes  $n$  points of a time-domain waveform into single points, and calculates the  $n$  frequency spectra corresponding to  $n$  time-domain waveforms [8]. The last step of the FFT approach is to

synthesize the  $n$  frequency spectra into a single frequency spectrum of the waveform. The time-domain current and voltage waveforms obtained before and after harmonics injection are given in figures 3 and 4 respectively. These waveforms are subjected to the FFT process of the TDS 1001B digital scope to obtain the frequency-domain waveforms.

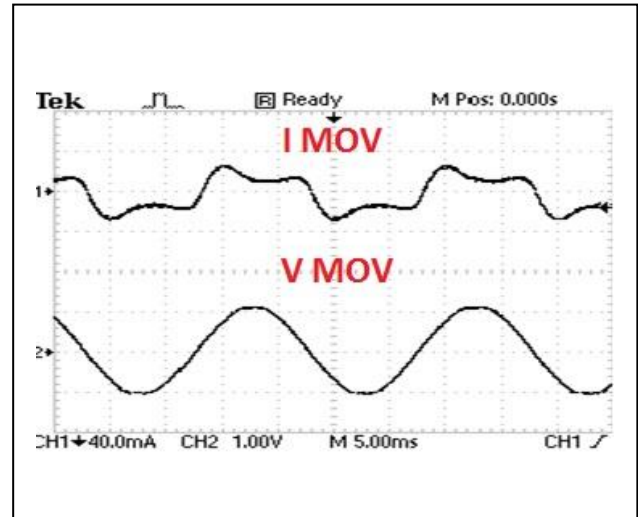


Figure 3: Time-domain current and voltage waveforms before supply distortion

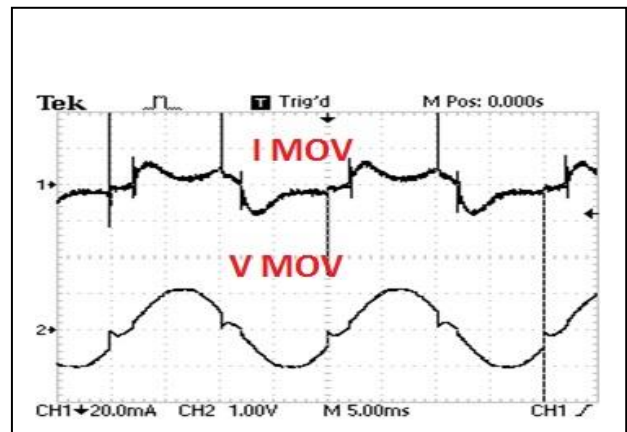


Figure 4: Time-domain current and voltage waveforms after supply distortion

### 4. AMPLITUDE OF THE THC

To estimate the percentage increase of the THC after harmonics injection, the amplitudes of the third harmonic components were measured in the frequency-domain of the current waveforms before and after harmonics injection conditions. Therefore, the flattop window was suitably selected on the FFT screen display of the scope. This enabled spectral leakage to be reasonably minimised in order to improve the accuracy of the amplitudes of the measured current components. Equation 1 enables the conversion from the frequency gain expressed in decibel (dB) into the rms value.

$$I_0 = I_i \cdot 10^{\frac{dB}{20}} \quad (1)$$

Where:

$I_0$  = the rms magnitude of output current

$I_i$  = the rms magnitude of input current

$dB$  = the current gain in decibel

The difference between the THC amplitudes obtained before and after distortion, which in fact indicates the change in terms of the external operating condition (switching of triac), is expected to be quite significant. Equation 2 enables the difference margin of the THC amplitudes to be quantified.

$$\Delta I = (I_A - I_B) \quad (2)$$

Where:

$I_A$  = the rms magnitude of current after harmonics injection

$I_B$  = the rms magnitude of current before harmonics injection

$\Delta I$  = change between the rms currents

## 5. RESULTS AND DISCUSSION

The typical time-domain waveforms of the varistor samples obtained before and after harmonics injection are given in figures 3 and 4 respectively. In the frequency-domain, the varistor waveforms before supply voltage distortion are depicted in figure 5.

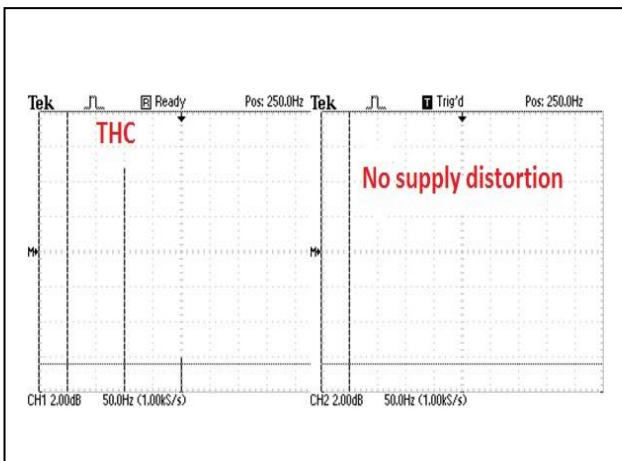


Figure 5: Frequency-domain waveforms before supply distortion

Under distortion conditions, the typical frequency-domain waveforms of the samples involved are given in figure 6.

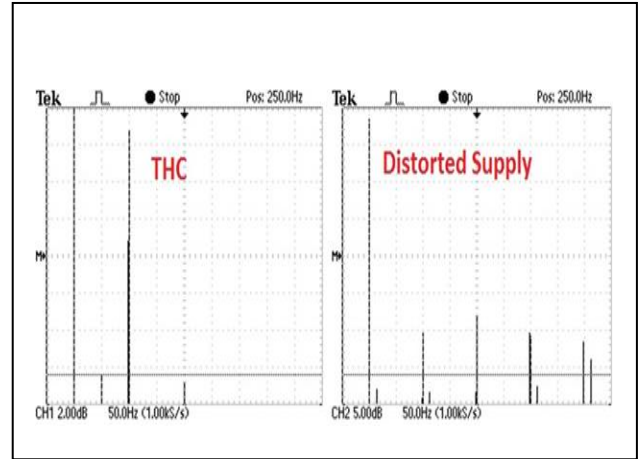


Figure 6: Frequency-domain waveforms after supply distortion

The time-domain waveform of the varistor current obtained before harmonics injection appears to be distorted. This is confirmed by the existence of harmonic frequencies in the frequency-domain spectrum of the current under the same experimental condition. After harmonics injection, the increase of the third harmonic amplitude is visible in the frequency spectrum. Out of the ten varistor devices used in the experiment, the increase in the THC amplitude is observed in nine samples while only one sample displayed no THC amplitude growth whatsoever after harmonics injection. On average the THC amplitude variation between the two experimental conditions is averaged at 28.2 %.

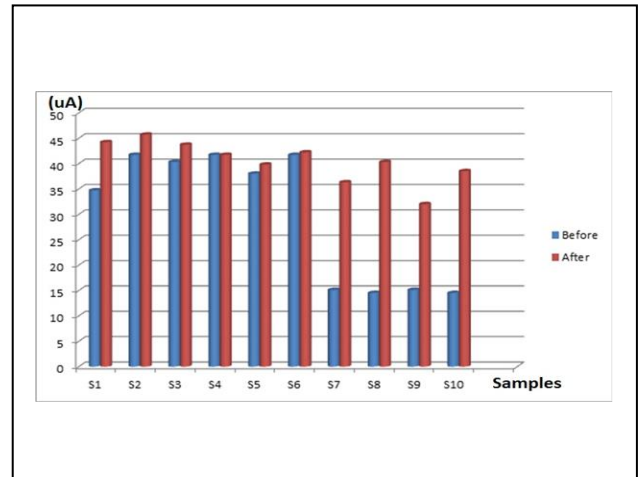


Figure 7: THC amplitudes before and after harmonics injection

It could also be noticed that 60 % of the samples studied showed marginal THC amplitude difference between the two experimental conditions. These samples could actually be degraded. The trend of the THC amplitudes for the samples before and after harmonics injection is shown in figure 7.

## 6. CONCLUSION

The time-domain waveform of the varistor leakage current, measured before and after harmonics injection, is decomposed in frequency-domain in order to verify the negative impact of distorted supply voltage on the THC-based condition assessment of varistor arresters. This study has demonstrated that a harmonic source, with predominant third harmonic components, providing distortion to the voltage across varistor units, causes the THC amplitude to increase. This increase in the THC is not necessarily indicative of the varistor condition.

## REFERENCES

- [1] V. Larsen and K. Lien: "In-service Testing and diagnosis of gapless metal oxide surge arresters", Proceedings: 9<sup>th</sup> *International Symposium on Lightning Protection*, Foz do Iguacu, November 2007.
- [2] F. Mahmood, M. Nadeem and U. Jamail: "A Comprehensive need of zinc oxide varistors in electronics technology", *Science Research Journal*, Vol. 18 No. 3, pp. 185-195, July 2007.
- [3] J. Woodworth: "Arrester condition monitors-A state of the art review", *Arrester Facts* 036, [www.arresterworks.com](http://www.arresterworks.com).
- [4] A. Karim, S. Begum and M. Hashmi: "Performance and failure during energy testing of zinc oxide varistor processed from different size fraction and passivation thickness", *International Journal of Mechanical and Materials Engineering*, Vol. 5 No. 2, pp. 175-181, October 2010.
- [5] M. Wang, Q. Tang and C. Yao: "AC degradation characteristics of low voltage zno varistors doped with Nd<sub>2</sub>O<sub>3</sub>", *Ceramics International*, Vol. 33 No. 2, pp. 1095-1099, November 2010.
- [6] M. Jaroszewsky, P. Kostyla and K. Wieczorek: "Effect of voltage harmonics content on arrester diagnostic result", *International Conference on Solid Dielectrics*, Toulouse, July 2004.
- [7] R. Herrera, P. Salmeron and S. Litran: "Assessment of harmonic distortion sources in power networks with capacitor banks", Proceedings: 11<sup>th</sup> *International Conference on Renewable Energies and Power Quality*, Las Palmas de Gran Canary, April 2011.
- [8] S.W. Smith: *The scientist and engineer's guide to digital signal processing*, pp. 141-241, [www.dspguide.com](http://www.dspguide.com).